Modeling the Buckling of Isogrid Plates

J. Lavin[1] and E. Gutierrez-Miravete[*,2]
[1]United Technologies-Pratt & Whitney, [2]Rensselaer at Hartford
*Corresponding author: 275 Windsor Street, Hartfrod, CT 06120, gutiee@rpi.edu

Abstract
Isogrid components are widely used in aerospace applications because they reduce weight while maintaining structural efficiency. This paper reports findings from an investigation on the buckling of isogrid plates. Isogrid plates can be regarded as flat plates strengthened by an appropriately designed superimposed grid structure of ribs (see figure 1).

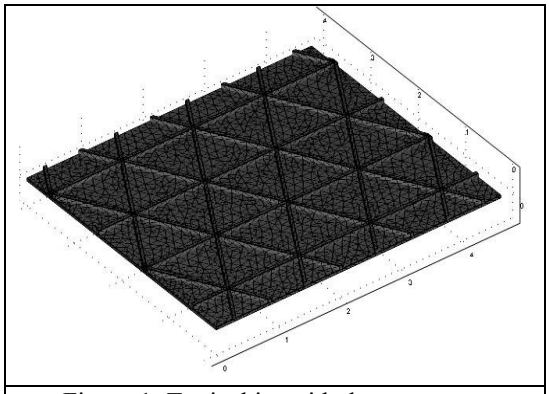

Figure 1: Typical isogrid plate structure

Finite element models of of both uniform thickness and isogrid plate structures are developed using COMSOL Multiphysics and the buckling behavior is compared with that obtained using analytical methods.

Keywords: Isogrid plates, deflection, buckling, modes.

1. Introduction
The design of the isogrid structure allows the component to maintain isotropic properties even though material has been selective removed for weight reduction. Most importantly, the reduction in weight is obtained without significant deleterious effects on stiffness. In applications, isogrid structures are subjected to a variety of boundary constraints and loading conditions all of which can vary during operation. Initial designs are completed with the best available predicted loads that must then be validated during engine testing. Even with advances in technology the predicted temperatures and pressures are not exact. These changes can vary the component load direction and orientation. In order to maintain structural integrity the isogrid must continue to function properly if load orientation changes during operation.

In designing isogrid structures the components are often simplified to a single sheet. This simplification was developed for NASA years ago and is known as the E^*t^* method [1]. The simplification process of the isogrid has been noted as a potential cause of component failure and is currently being reviewed. The component is designed to sustain specific boundary conditions (e.g. load directions, magnitudes and constraints). The change in load direction is also a potential cause of failure. For this reason, three different load orientations are investigated in this report to ensure the load orientation relative to the isogrid is not a reason for failure.

2. Methodology
Once the plate characteristics and boundary conditions are defined, a closed form solution is evaluated for each loading condition. Corresponding finite element models are then created for comparison to the closed from solution. The E^*t^* method is used to simplify the isogrid to a plate. This simplification is used as an input to the analytical solution as well as used in a numerical analysis of the plate. These two solutions are compared to ensure proper boundary condition modeling technique as well as to determine an appropriate mesh density. The plate model will also be used for comparison to the modeled isogrid geometry. All numerical models are created using the COMSOL finite element code.

In COMSOL both a static solution and a linear buckling solution are obtained. The static solution is reviewed to verify the input load has the correct magnitude and that the initial conditions do not impart any additional constraint. Upon verification of the boundary conditions and input loads the linear buckling analysis is completed. This analysis is

completed with a unit load (verified in the static solution) so that the calculated eigen-value is the critical buckling load. These loads are then compared to the analytical solution for verification of the E^*t^* methodology. Analytical buckling mode shapes are also compared to numerically computed mode shapes of the plate and isogrid to ensure consistency.

Isogrid structures are typically cumbersome to model and multiple iterations are needed to obtain the correct stiffness required in the design. Thus it saves design iteration time if the structure can be turned into an equivalent single sheet with representative stiffness. The plate will not have the same geometric dimensions as the isogrid but it will have the same stiffness in both the tensile and bending directions. This simplification allows multiple design iterations to be completed by changing only the stiffness of the part and not the model geometry. The simplification also allows for a reduction in computational time. A detailed description of the analytical formulation used to obtain closed-form solutions for buckling of isogrid structures using the E^*t^* method together with references to the appropriate literature can be found in [2].

3. Analytical Solutions

The first case is a simply supported plate in uni-axial compression. The plate was 1" x 1" with a thickness of .040". The second case used was a 1.000" x 1.1547" plate with a thickness of .046". This thickness is derived from the isogrid cross-section geometry shown in figure 2 and the equations presented [2]. The isogrid is representative of the geometry found in a failing component. The face sheet thickness is .030" and the ribs are .050" tall by .040" wide with a triangle side length (*a*) of 1.154" and a triangle height (*h*) of 1.000". The two cases will be used to verify the numerical results for a plate with varying height to width ratio as well as thickness.

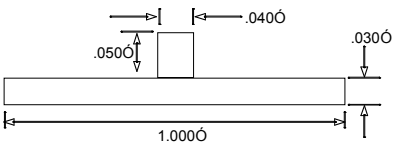

Figure 2: Isogrid geometry

The plate has all edges simply supported. The free body diagram in figure 3 is similar to a section of the component in which the suspected change in boundary conditions is being observed. The component is free in the y direction and the load is known in the x direction.

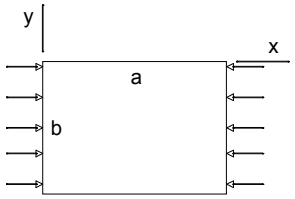

Figure 3: Free body diagram

The buckling load for this problem is calculated using the closed form solution. The critical value will occur with *n* equal to 1, where both *m* and *n* are integers. The value of *m* corresponds to the number of half waves parallel to the direction of loading while *n* determines the number of half waves perpendicular to the direction of loading. The material properties used in all calculations are shown in table 1 and the calculated first 5 critical buckling loads are shown in table 2.

E^*	$20.83e^6$ psi
ν	.3

Table 1: Material Properties

1.000Ó x 1.000 ÓPlate			1.000Ó x 1.1547Ó Plate b = 1.000		
$F_{critical}$ (lb)	m	n	$F_{critical}$ (lb)	m	n
4818	1	1	7529	1	1
7529	2	1	9833	2	1
13385	3	1	16406	3	1
19274	2	2	25966	4	1
21758	4	1	30115	2	2

Table 2: Critical buckling loads (cases 1 and 2)

From the results in table 2 it is seen that the mode shapes of the plate change as a function of the ratio of a/b. This can be seen by the change in critical load and the values of m and n between the fourth and fifth values of the calculated examples.

The third case investigated involved a change in orientation of the loading on the plate. For the

1x1 plate there is no change in critical buckling loads but for the rectangular plate of case 2 (1.000 x 1.1547) there is a change to the critical loads. Again this is caused by the ratio of a/b and the change in load orientation. The comparison of calculated loads can be seen in table 3.

Load on edge *a* a = 1.000"			Load on edge *b* b = 1.1547"		
$F_{critical}$ (lb)	m	n	$F_{critical}$ (lb)	m	n
6520	1	1	7529	1	1
12008	2	1	9833	2	1
22487	3	1	16406	3	1
26080	2	2	25966	4	1
34064	3	2	30115	2	2

Table 3: Buckling load/mode change with edge loading (case 3)

Additionally the critical loads were calculated for loading on both of the edges of the plate. This load case is most similar to the loading of the failing part in the field. The additional load on the plate further reduces the load required to buckle the plate.

This final load case has a solution shown in equation 1. Again the values of *m* and *n* change the mode shape and the critical load required to produce buckling in the plate. As expected the combined load case has reduced the critical value below the previous two load cases. The calculation of the critical values can be seen in table 4.

$$P_x = \frac{\left[(mb/a)^2 + n^2\right]^2}{(mb/a)^2 + (P_y b/P_x a)n^2}\frac{\pi^2 D}{b} \quad [1]$$

Calculated (lb)	Kcc	m	n
3494	1.9	1	1
9872	5.4	1	2
7631	4.1	2	1
13976	7.6	2	2
14541	7.9	3	1

Table 4: Critical values for loading on both edges of 1.000 x 1.1547 plate (case 4)

Each of these load cases will be compared to the simplified isogrid structure to determine the applicability of the E^*t^* method.

4. Finite Element Modeling

COMSOL was used to model the buckling of the isogrid plate and that of the equivalent plate. The results in this section are then compared to the analytical solutions from the previous section to determine the validity of both models. The numerical results are also compared to each other to ensure the use of the equivalent plate method will provide similar numerical answers to the isogrid model.

Each model created is used to first compute a static solution prior to calculating a buckling solution. This is required so that COMSOL can calculate the pre-stress in the model. The pre-stress is required for the calculation of the stiffness matrix needed in the eigen-value buckling solution.

Four different models were created to verify the applicability of the E^*t^* method. Each model was created using the gravitational IPS units. The two main variables elastic modulus (E and E^*) and thickness (t and t^*) have units of psi and inches.

The first model created was a 1.000" x 1.1547" x 0.046" plate. The plate model was used to compare the results of the COMSOL modeling technique to those obtained from the analytical solution. The plate is a constant thickness (t^* = 0.046") and given modulus of elasticity (E^* = $20.83e^6$ psi).

To match the plate model described above a single isogrid panel was created for comparison. The geometry was created using a single block (1.000" x 1.1547" x 0.030") and adding individual ribs. The ribs were created at the center of the plate and then rotated 60° about the center in either direction. Each rib was 1.500" x 0.040" x 0.050". These ribs were then trimmed with separate blocks to create the proper length. The final rib was then created at the center of the plate and formed the last piece of the isogrid.

The third model created was a 4.000" x 4.618" x 0.046" plate. The plate was again modeled from the simplification of the isogrid, which required a constant thickness (t^*) of 0.046". The modulus of elasticity (E^* = $20.83e^6$ psi) used was also the

same as the original 1.000" plate and calculated using the $E^* t^*$ process.

The final model created was an isogrid geometry 4.000" x 4.618" that maintained the same rib length (a) and height (h) of the initial 1.000" model but contained more isogrid cells. The model was created using a similar technique to the first model but after rotating the diagonal ribs each rib was arrayed in the x direction to create multiple entities from the original. The array process allowed for a reduced number of modeling steps. Once the rotated ribs were created the final horizontal ribs were added and united to the rotated ribs. Creating a composite object of just the ribs allowed for a reduction in the number of subtractions required to create diagonal ribs with the proper length. The model now had two components. The face sheet of constant thickness and the rib structure were left as separate entities so that a rib height variation could also be completed.

The rib height study models were each created separately by scaling the ribs of the original isogrid model in the z direction. This allowed for the face sheet thickness to remain unchanged for each separate analysis so that only a change in rib geometry was evaluated.

The isogrid dimensions seen in figure 4 were used along with the procedure described in [2] to produce the appropriate thickness (t^*) and modulus of elasticity (E^*). The computations were completed in excel to simplify the calculation effort. Table 5 shows the comparison of thickness and elastic modulus.

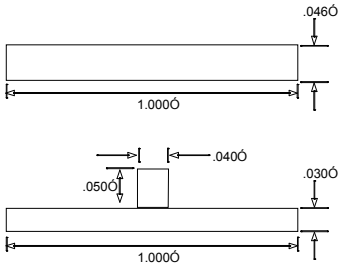

Figure 4: Plate and isogrid cross section

	Thickness	Elastic Modulus (lb/in^2)
Plate	.046"	$20.83e^6$ (E^*)
Isogrid	As drawn	$30.00e^6$ (E_0)

Table 5: Material property comparison

The boundary conditions for the isogrid were identical to the plate. Each side of the isogrid is simply supported to match the analytical solution constraints. This requires support in the vertical z direction with additional constraints at specific points in order to prevent a rigid body motion. The point constraints are at the center of each edge and constrain movement in the direction parallel to the edge.

The geometry from the 1.000" x 1.1547" model of both the equivalent sheet and the isogrid were meshed with tetrahedral 3D quadratic elements. The isogrid mesh contained 25423 elements and 126690 degrees of freedom. The analytical solution of a plate with a single edge load produces a critical buckling load of 7529 lb. The critical buckling load for the isogrid finite element model was computed at 6735 lb and the finite element model of the plate calculated a critical buckling load of 7180 lb. This is within 10.5% and 4.5% respectively of the analytical solution for a flat plate of equivalent stiffness.

These predictions were not considered acceptable for verification of the equivalent stiffness method so a larger 4.000" x 4.618" model was evaluated to remove the influence that the boundary conditions may have on the results. Therefore a sequence of increasingly refined models was developed.

The final model previously descried was a rectangular panel with the same isogrid pattern as the small model. The lengths a and h for the isogrid were kept the same so that the $E^* t^*$ simplification did not change between the small and large models. The isogrid simplification reduces the system to a unit width, which remains applicable to the larger system, provided the geometry is produced properly. All final results and comparisons presented will be from the larger 4.000" x 4.618" model.

The isogrid model mesh, boundary conditions and loads can be seen in figures 5-7. The final mesh consisted of 16358 elements and 96660 degrees of freedom. The free mesh parameters were set to "coarser" to create the mesh. A study was completed using the "extremely coarse" and "extra coarse" free mesh parameter option.

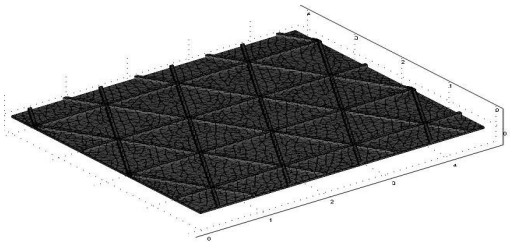

Figure 5: Final isogrid geometry

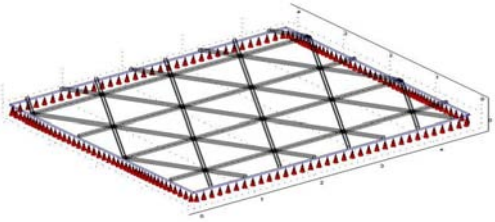

Figure 6: Final isogrid boundary conditions

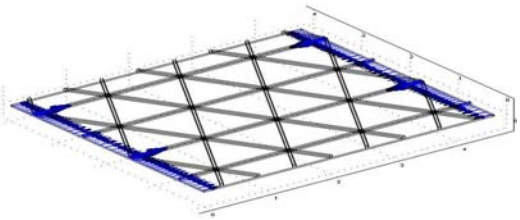

Figure 7: Final isogrid load (case 1)

Element count versus percent error to the first critical buckling load is shown in table 6.

Model	Element Count	Analytical Solution (lb)	First Critical Buckling Mode (lb)	Percent Error
Isogrid	6716	1882	2049	8.86
	10076	1882	1972	4.77
	16358	1882	1946	3.39
Plate	4408	1882	1870	-.65
	7668	1882	1862	-1.07
	12203	1882	1858	-1.28
	17432	1882	1857	-1.33

Table 6: Effect of Number of Elements on the computed critical Buckling Loads

A similar study was also completed for the plate model. The model was run with the "coarser", "coarse", "normal" and "fine" free mesh parameters. This study showed that the model converged to a solution and the "normal" free mesh parameter was used. This produced a model with 12203 elements. Unlike the isogrid model, the plate model under-predicts the first critical buckling load.

As the element count increased the accuracy of the solution increased. A graph of the data from table 6 readily shows that the slope changes little with the number of elements once ~10000 elements are used. The final element count provided accurate results while allowing the model to be solved in approximately 5 minutes.

The boundary conditions were again applied to approximate a simply supported plate and boundary loads were applied to the main face of both the plate and isogrid. The loads were applied to the boundary face and applied so that the total input load was 1 lb per each side.

To ensure the E^*t^* isogrid simplification method produces accurate critical loads all three load cases were run with the 4.000" x 4.618" size isogrid model. This will also provide substantiation that load orientation into the isogrid can be neglected. Models were created with loads applied to additional faces (not shown in figure 7) to simulate the load cases discussed in the previous section. This included loading on the long edge and both edges.

A comparison of the buckling mode shapes and the corresponding loads are shown in table 7 for the 4.000" x 4.618" plate with loading on edge b. As the mode shapes increase in complexity the accuracy of the model does not reduce. This shows the model is capable of predicting accurate displacement with the mesh. For the loads applied to edge b the first 4 modes should correspond to $m = 1 \rightarrow 4$ with the value n remaining constant at n = 1. The fifth mode being the first mode were the value of n = 2.

Calculated	Percent Error	Comsol Plate	m	n
1882	-1.28	1858	1	1
2458	-1.11	2431	2	1
7529	-1.27	7433	2	2
4102	-0.94	4063	3	1
6492	-0.87	6435	4	1

Table 7: 4.000" x 4.618" Critical load (lb) on edge b

To ensure the model could capture the change in geometry (i.e. non-square) and load orientation, the model was run with a load applied to edge *a* (long edge). The error results are similar to the model with load applied to edge b. This showed the isogrid model and the E^*t^* method accurately predicted loads with a changing length ratio.

The model was also evaluated for loading applied to both sides (*a* and *b*) of the plate and the solution was compared to the analytical value using equation 1. The results compared well to the analytically calculated value as shown in table 8.

Calculated	Percent Error	Comsol Plate
874	-0.75	867
2468	0.13	2471
5128	1.38	5199
1908	0.02	1908
3494	0.71	3519
3635	1.18	3678
5215	-2.07	5107

Table 8: 4.000" x 4.618" Critical load (lb) on edges a and b

The 4.000" x 4.618" COMSOL isogrid results were compared to the E^*t^* analytical solution and the COMSOL plate. The model for the COMSOL isogrid accurately predicted the critical buckling loads as compared to both the analytical value and the COMSOL plate model.

The final case used to verify that the E^*t^* method accurately calculates critical buckling load is the combined loading on both edge *a* and edge *b*. This load case also produces critical buckling loads similar to both the plate numerical and analytical analysis. The result for the model with loads applied to both edges is seen in table 9.

Calculated	Percent Error	Comsol Plate	Isogrid	Percent Error	m	n
874	-0.75	867	902.00	3.26	1	1
2468	0.13	2471	2556	3.57	1	2
1908	0.02	1908	1971.00	3.32	2	1
3494	0.71	3519	3532.00	1.08	2	2
3635	1.18	3678	3737.00	2.80	3	1

Table 9: Isogrid model critical loads (lb) comparison, load applied to both edges

Despite accurate critical loads being calculated, the mode shape of the linear buckling solution must be verified in order to ensure there are no modeling issues present. These issues can arise due to imperfections in the model geometry, boundary conditions or from anti-symmetric loads. They can also arise from abrupt stiffness changes that may be seen in the transition between the skin thickness and the ribs.

Thus the final step to verifying the E^*t^* method is to compare the predicted mode shapes for the isogrid geometry with the mode shapes produced by the plate model and the analytical solution. Each mode produced from the isogrid model is compared to the plate model to verify the shapes are correct. The plate models can be compared to the analytical solution with specific values of *m* and *n* to determine if they are accurate. As an example, figure 8 shows a mode shape comparison for the combined loading condition.

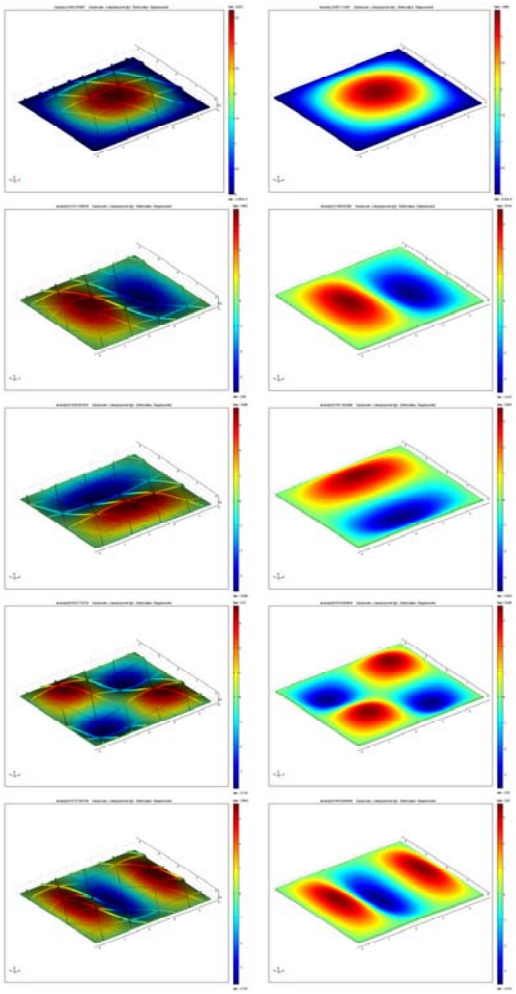

Figure 8: Isogrid and plate model mode shape 1-5 comparison loaded on both edges

Changing rib geometry relative to the plate changes the critical buckling loads without changing the buckling mode shapes until the ribs begin to dominate the stiffness of the structure. An example of the change in buckling mode shape for varying rib geometry can be seen in figure 9. This change in failure mode signifies when the E^*t^* method is no longer applicable to use to determine the critical buckling load or mode shape of the part.

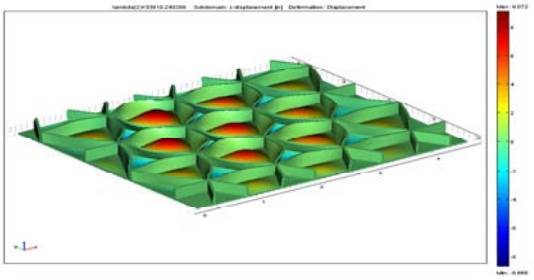

Figure 9: Example of rib buckling mode

To determine the change in mode shape with respect to rib geometry a single load case was completed with loads applied to both edge a and edge b. Four different rib geometries were modeled with an increasing height. The width of the rib, height of the isogrid triangle and the skin thickness is all held constant.

As stated previously, the ribs were created in the COMSOL model as one composite object and the skin was created as a separate object, which allowed for rib scaling in the z direction. For each new model a new value of E^* and t^* are calculated for use in the analytical solution. Each model was then compared to the analytical solution for verification of the critical buckling load. Additionally the mode shapes for each geometry change are evaluated to ensure the failure mode did not change from plate buckling to rib buckling.

5. Conclusions

COMSOL accurately predicts both the critical buckling loads and mode shapes for simply supported flat plates. Several models of varying size were compared to analytical solutions and the final results were within 2%. There is good correlation between the two solution techniques. The 4" x 4.618" plate numerical model under-predicts the buckling load relative to the analytical solution by approximately 1.3%, while the isogrid model over-predicts the critical buckling load relative to the analytical solution by approximately 3.5%. The plate model is converged and it is assumed that with additional computational resources the isogrid model error could be reduced. This is shown in the comparison between element count and percent error for the isogrid model. This comparison and correlation provides the basis for using COMSOL to predict the validity of the E^*t^* method.

The model was completed as a full symmetry model for all cases to ensure the proper boundary conditions were established. Initially the model was completed with a symmetry boundary condition on two sides to simplify the modeling constrain. Upon comparison to the analytical solutions and the full symmetry model the symmetric model did not produce answers that matched either the analytical solution or the full symmetry numerical solution. It was assumed that the symmetry modeling constraints were either incorrectly applied or calculated incorrect loads and mode shapes. No further investigation was completed into why the symmetric model did not compare favorably to the analytical or full symmetry solutions.

Regarding mode shapes, COMSOL correctly produced the first five mode shapes when compared to the analytical solution. Only when buckling of the ribs occurred were incorrect mode shapes produced. The incorrect mode shapes were used to determine the applicability of the E^*t^* method to the geometry.

6. References

[1] McDonnell Douglas Astronautics Company. 1973. *Isogrid Design Handbook*. CA. McDonnell Douglas Astronautics Company.

[2] J. Lavin, Buckling of Isogrid Plates, Master of Engineering Project Report, Rensselaer at Hartford, June 2010. Available online at http://www.ewp.rpi.edu/hartford/~lavinj/